Effect of Protein Dynamics upon Reactions that Occur in the Heme Pocket of Horseradish Peroxidase†

Mazdak Khajehpour,‡ Thomas Troxler,§ and Jane M. Vanderkooi*,‡

Department of Biochemistry and Biophysics, School of Medicine, and Regional Laser and Biotechnology Laboratories, Department of Chemistry, University of Pennsylvania, Philadelphia, Pennsylvania 19104

Received April 30, 2002

ABSTRACT: Free base and Pd porphyrin derivatives of horseradish peroxidase show long-lived excited states that are quenched by the presence of the peroxidase inhibitor, benzhydroxamic acid. The relaxation times of the excited-state luminescence and the rates of the quenching reaction for these derivatives of peroxidase were monitored as a function of pH, temperature, and viscosity with the view of examining how protein dynamics affect the quenching reaction. As solvent viscosity increases, the rate decreases, but at the limit of very high viscosity (i.e., high glycerol or sugar glass) the quenching still occurs. A model is presented that is consistent with the known structure of the enzyme−inhibitor complex. It is considered that the inhibitor is held at an established position but that solvent-dependent and independent motions allow a limited diffusion of the two reactants. Since there is a steep dependence upon distance and orientation, the diffusion toward the favorable position for reaction enhances the reaction rate. The solvent viscosity dependent and independent effects were separated and analyzed. The importance of internal reaction dynamics is demonstrated in the observation that rigidity of solvent imposed by incorporating the protein into glass at room temperature allows the reaction to occur, while the reaction is inhibited at low temperature. The results emphasize that protein dynamics plays a role in determining reaction rates.

For most protein-catalyzed electron transfer reactions, a redox active group reacts with another protein bound molecule or moiety that is located at a distance much larger than the distance of van der Waals contact. Because the electron transfer is exponentially dependent upon the distance, distance is a major determinant of the rate of transfer (*1*−*3*). Intervening atoms also play a role (*4*, *5*). For donor and acceptor moieties located in proteins, an additional factor is that their approach toward one another is a function of the protein dynamics.

Proteins are flexible molecules that undergo both large and small amplitude motions. In terms of phase space, this flexibility implies that there exist many local minima along the energy surface of a protein (*6*). Transitions between the different local minima of the proteins belong to the class of solvent phase reactions (*7*). Since the reactants are, in effect, in a bath that consists of the protein polypeptide chain and the solvent, the reactants have many modes of vibration to exchange energy. For this reason, transition state theory is not applicable. Kramers addressed this problem of transition state theory for the effect of viscosity on a uni-molecular in a solvent and demonstrated that solvent friction (as characterized by its viscosity) has an influence upon the rate constant (*8*). Kramers' theory has been applied extensively to condensed phase kinetics, and a recent review by Tucker (*9*) gives an idea of an application of this theory.

Our system of interest is the enzyme horseradish peroxidase (HRP)[1]. HRP consists of a heme that is bound to the apo-protein via hydrophobic interactions. HRP catalyzes the oxidation of a wide variety of aromatic molecules (AH_2). The mechanism of oxidation of aromatic compounds is (*10*−*12*)

$$\mathrm{HRP} + \mathrm{H_2O_2} \leftrightarrow \mathrm{HRP{-}H_2O_2} \rightarrow \mathrm{HRP\text{-}I}$$

$$\mathrm{HRP\text{-}I} + \mathrm{AH_2} \leftrightarrow \mathrm{HRP\text{-}I{\bullet}AH_2} \rightarrow \mathrm{HRP\text{-}II} + \mathrm{AH}\bullet$$

$$\mathrm{HRP\text{-}II} + \mathrm{AH_2} \leftrightarrow \mathrm{HRP\text{-}II{\bullet}AH_2} \rightarrow \mathrm{HRP} + \mathrm{AH}\bullet$$

$$2\mathrm{AH}\bullet \rightarrow \mathrm{A_2H_2} \text{ or } \mathrm{A} + \mathrm{AH_2}$$

where HRP-I (compound I) and HRP-II (compound II) are spectroscopically distinct intermediates. An inhibitor that binds tightly to HRP is benzohydroxamic acid (BHA). Schonbaum first systematically studied this inhibitor (*13*) in pioneering work that laid the foundation of further studies (*12*, *14*−*30*). BHA binds to HRP in a manner similar to the HRP substrates and is a competitive inhibitor for the HRP enzymatic reaction (*29*). Its binding specificity arises because

† This work was supported by NIH PO1 48130 and NIH RR 01348.

* To whom correspondence should be addressed. Phone: (215) 898-8783. Fax (215) 573-2085. E-mail: Vanderko@mail.med.upenn.edu.

§ Regional Laser and Biotechnology Laboratories, Department of Chemistry, University of Pennsylvania.

‡ Department of Biochemistry and Biophysics, School of Medicine, University of Pennsylvania.

[1] Abbreviations: HRP, horseradish peroxidase; MPHRP, mesoporphyrin-IX substituted horseradish peroxidase; Pd-MPHRP, palladium bound mesoporphyrin-IX substituted horseradish peroxidase; BHA, benzohydroxamic acid.

10.1021/bi020325n CCC: $25.00
Published on Web 02/14/2003

of the fact that it can form three hydrogen bonds to the Arg38, His42, and Pro139 residues in HRP (*27*).

Emission spectroscopy provides a powerful tool to probe environmental interactions as molecules in the excited state are much more reactive than in the ground state (*31*). However, the heme in the native state of HRP contains an iron that effectively quenches emission from the excited state. To utilize emission spectroscopy, it is necessary to modify the heme group in HRP such that it has a long emission lifetime. The use of substituting the heme in HRP with fluorescent porphyrin analogues and studying the effects of BHA binding upon the porphyrin emission spectrum was first demonstrated by Aviram (*14*). Aviram demonstrated that BHA both quenches and modifies the steady-state spectrum of the fluorescent porphyrins that he studied. Horie et al. (*15*) studied the effects of BHA upon the photochemical relaxation of the excited singlet and triplet states in porphyrin substituted HRP and showed that the excited triplet state is more quenched than the singlet state.

In this paper, we modify the heme group of HRP by exchanging the heme prosthetic group of HRP with mesoporphyrin-IX (MPHRP) and with Pd-mesoporphyrin-IX (Pd-MPHRP). These groups were chosen because of their unique photochemical properties. The modified protein MPHRP demonstrates fluorescence with high quantum yield from the excited singlet state. The Pd-MPHRP derivative of HRP has to our knowledge not been prepared before. This derivative was prepared based upon our knowledge of Pd substituted porphyrins (*32*, *33*). Palladium derivatives of porphyrins have a very large phosphorescence quantum yield, with a greater than 99% conversion to the excited triplet state. This large signal provides good time resolution for lifetime measurements.

The reaction that we have utilized as a probe of protein dynamics is the simple photochemical reaction of quenching of the excited triplet state of the porphyrin system by the bound BHA. Excited-state quenching is a nonlinear function of the distance and also an orientation dependent process (*34*). When the optically excited species and the quencher are both moieties bound to the protein, the quenching rate of the excited species can potentially depend on the protein dynamics. To understand the protein dynamic effects, it is critical to elucidate the processes involved in the photochemical relaxation of the excited-state porphyrin moieties in this protein system. This has been accomplished by performing a series of excited triplet state lifetime measurements upon the modified HRP proteins. We have investigated the effects of temperature, pH, and deuterium substitution upon the excited triplet state lifetimes of the protein in both the unbound and the bound to BHA states. The protein dynamics has been investigated by measuring the viscosity dependence of the quenching rate constant. To this end, we have measured the temperature dependence of the quenching reaction in a series of glycerol−water mixtures and in a trehalose−sucrose glass system. We demonstrate that increasing the viscosity can slow the reaction but that at the limit of very high viscosity (glass state) the quenching can still occur. These results indicate that fluctuations in the heme pocket are modulated by solvent, and these fluctuations are due to the long amplitude breathing motions of the protein.

MATERIALS AND METHODS

Materials. Benzohydroxamic acid (BHA) was obtained at 99% purity from Aldrich (Milwaukee, WI) and used without further purification. BHA was introduced into the aqueous media by preparing a 0.064 M solution in absolute ethanol and adding the solution to the sample. HRP in the native state was obtained from Sigma (St. Louis, MO). Mesoporphyrin-IX (MP-IX) and Pd-mesoporphyrin-IX were obtained from Porphyrin Products (Logan, UT), and they were incorporated into HRP to form MPHRP and Pd-MPHRP via the methodology described previously (*35*). The protein concentrations in the samples were 25 μM, and the BHA concentration was 250 μM, except where indicated. The solutions were deoxygenated via an enzymatic reaction. Glucose, glucose oxidase, and catalase were obtained from Sigma and used for deoxygenation via known protocols (*36*). The sugar glass was made by combining trehalose, sucrose, and water in a 1:1:2 ratio and heating the mixture to 60 °C (*37*). The solution was then cooled to 30 °C, and the protein was added. The highly viscous sugar solution was laid on a quartz plate and placed in a desiccator under vacuum in the dark for 2 days in order for the sugar glass to form by evaporation of the water. The glass was optically clear with no indication of crystal formation.

Steady-State and Triplet-State Measurements. All measurements were performed in a Fluorolog-3 Spex instrument equipped with a 928 Hammamatsu photomultiplier tube. Triplet state measurements were performed utilizing a Spex 19340 phosphorimeter module coupled to the Fluorolog-3 instrument. All spectra were corrected for lamp fluctuations. The results were analyzed by utilizing commercially available software, Sigmaplot (Chicago, IL).

Nanosecond Measurements. Time-resolved fluorescence decays were measured at the Regional Laser and Biotechnology Laboratories facility at the University of Pennsylvania. The sample was placed in a temperature controlled quartz cell (Starna Cell 62-F-Q-10). Excitation at 408 nm was achieved using a fixed frequency pulsed-diode laser (PDL 800-B from PicoQuant, Germany) set to a 4 MHz repetition rate. Fluorescence emission was collected at magic angle and detected at 620 nm using a MCP-PMT (Hamamatsu R3809U) at the output slit of a subtractive double monochromator. Decay curves were obtained by a time-correlated single photon counting technique with a bin size of 113 ps over an approximately 50 ns period following excitation. The intensity decay data were analyzed using the LIFETIME program allowing time constants, preexponential amplitudes, constant background, and a time shift between prerecorded instrument function and decay curve to vary as free parameters. Typical overall instrument response was 120 ps fwhm.

Analysis. In Figure 1, we have depicted the photochemical relaxation mechanism of the porphyrin moiety in the HRP derivatives. If the formation of the triplet state is much more rapid than the decay, the lifetime of the triplet state τ is defined as $\tau = 1/(k_e + k_m + k_p + k_q[Q])$ in which [Q] is concentration of quencher, and all other quantities are defined in Figure 1. In the case of BHA, since it is a bound substrate to the protein, the concentration of quencher is constant enabling us to define an apparent quenching rate constant $k' = k_q[Q]$. In this case, if τ_0 is the triplet state lifetime in the absence of quencher and τ is the lifetime in the presence of

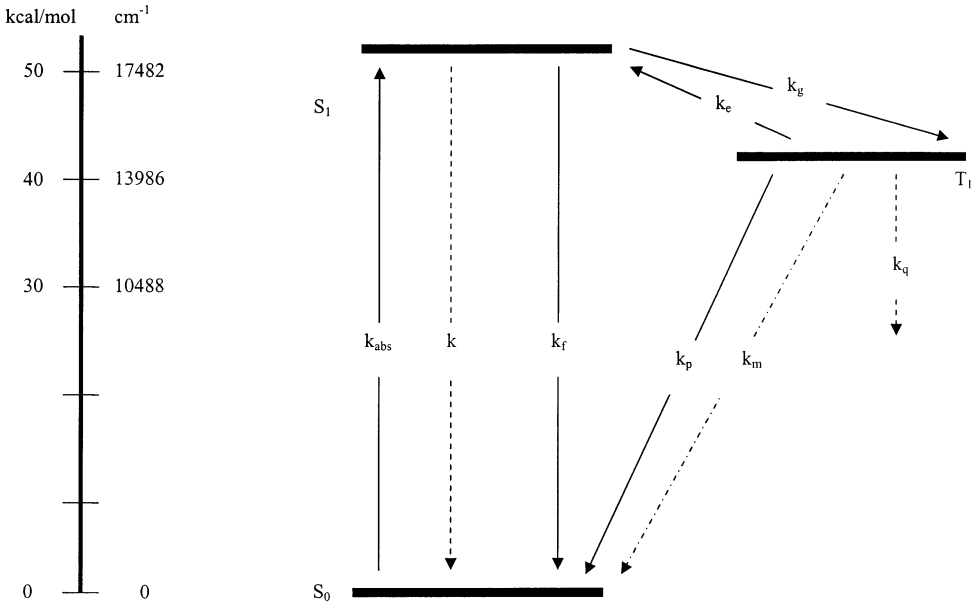

FIGURE 1: Energy diagram of the photochemical decay of the singlet and triplet excited states of Pd-MPHRP. In this figure, k_{abs} is the rate for the absorbance, k is the nonradiative decay rate for the excited singlet state, k_f is the rate of fluorescence decay, k_g is the S_1 to T_1 intersystem crossing rate, k_p is the rate of phosphorescence decay, k_e is the T_1 to S_1 intersystem crossing rate, k_m is the nonradiative intersystem crossing rate between T_1 and S_0, and k_q is the quenching rate.

the quencher, then k' is given by

$$k' = \tau^{-1} - \tau_0^{-1} \quad (1)$$

The quenching reaction depends on the distance and orientation of the reacting moieties relative to each other (*34*). Since both porphyrin and BHA are tightly bound to the protein, the approach of these groups toward each other is coupled to the protein motion.

Judging from the crystal structure, the BHA and porphyrin moieties in the protein are approximately 0.4 nm relative to each other (*23*). Thermodynamic considerations dictate the optimal binding structure of BHA to the protein. The most stable thermodynamic structure is not necessarily the most optimal for quenching as the optimal distance for quenching is the closest possible approach of the two moieties, and any protein motion causing BHA and porphyrin to approach one another closer should cause the quenching to be enhanced. Generally speaking, the distance dependence of energy transfer (which quenching is a form of) is normally expressed in terms of a generalized position coordinate (*2*). In effect, energy transfer not only depends on the distance between the two energy transferring species but depends on the angular orientation of the two species relative to each other as well.

To understand this, let us consider a simplified microscopic view of the motion of the quencher and phosphor relative to each other. Figure 2 is a scheme of the quenching process. Quenching is a distance dependent process that enables us to define a sphere of action; this is the area in which the intrinsic quenching rate is very fast as compared to other rate processes. Therefore, the quenching rate depends on the frequency that the quencher enters the sphere of action. Let us emphasize that the distance vector in Figure 2 is the generalized position coordinate (i.e., entering the sphere of action might not only involve a change in distance but may also involve a change in the orientation of the two moieties relative to each other).

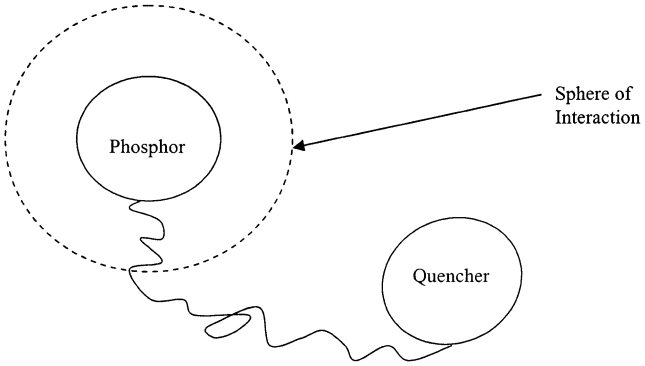

FIGURE 2: Scheme depicting the motion of the BHA and Pd-MP relative to each other inside a protein. The dynamic component of the quenching depends on the frequency that BHA enters the sphere of interaction.

Proteins have dynamic structures and undergo conformational fluctuations or breathing motions. Considering that both BHA and Pd-MP are tightly bound to the protein, the frequency that the BHA enters the interaction sphere is a function of protein motion. This motion can involve motions that are coupled to the solvent and can also involve motions that are solvent independent. At high viscosity, the protein is stuck in its equilibrium conformations, and the high viscosity prevents the protein conformations from interconverting, therefore abolishing the breathing motions of the protein. At high viscosity, the quenching is due to the solvent independent motions that exist in the heme pocket. Therefore, the solvent dependent component of the quenching reaction (which is solvent dependent) can be isolated via

$$k'' = k' - k_\infty \quad (2)$$

In this equation, k' is the measured quenching rate constant from eq 1, and k_∞ is the quenching rate constant measured in high viscosity solvents. The rate constant k'' characterizes the rate that solvent coupled protein motion brings BHA within the interaction sphere of the Pd-MP.

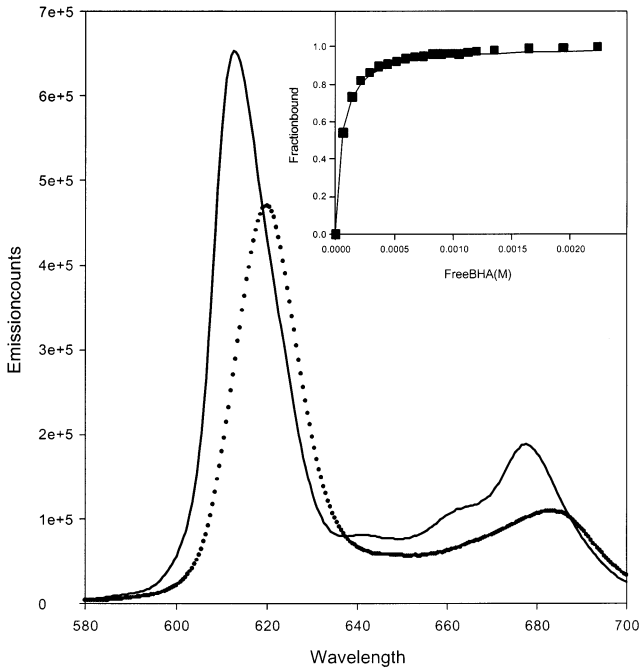

FIGURE 3: Steady-state emission spectra of MPHRP at room temperature in the absence (solid) and with 250 μM BHA. The experiment conditions were as follows: the protein concentration was 25 μM, the solvent was pH 5 ammonium acetate buffer (50 mM), the excitation wavelength was 400 nm, and the band-pass widths were set at 2 nm for excitation and emission. In the inset, the binding of BHA to HRPMP-IX at 1 °C is shown. The solid curve in the inset is the simulation of a binding curve having the complex dissociation constant $K_d = 51$ μM, while the full symbols are the experimental data.

We will now formulate this qualitative picture in terms of Kramers theory (*8*). In this case, $k'' = C/f \exp(-E_a/RT)$ where f is the friction coefficient, and E_a is the activation barrier. However, based upon the work of Ansari et al., the friction coefficient f in protein media can be broken into the $f = f_{protein} + f_{solvent}$ equation (*38*).

$$k'' = \frac{C}{f}\exp\left(-\frac{E_a}{RT}\right) = \frac{C}{f_{protein} + f_{solvent}}\exp\left(-\frac{E_a}{RT}\right) = \frac{C}{f_{protein} + a\eta}\exp\left(-\frac{E_a}{RT}\right) \quad (3)$$

where a is a proportionality constant. Rearranging eq 3, we obtain the following linear relationship in isothermal situations.

$$(k'')^{-1} = \frac{a\eta}{C\exp\left(-\frac{E_a}{RT}\right)} + \frac{f_{protein}}{C\exp\left(-\frac{E_a}{RT}\right)} = M\eta_{solvent} + N \quad (4)$$

in which M and N are constants. Therefore, if k'' is highly coupled to long-range protein motions, the linear relationship of eq 4 should be obtained. The internal friction of the protein increases with decreasing temperature; therefore, the ratio N/M should increase as the temperature drops.

RESULTS

Photochemical and Spectroscopic Results. Figure 3 demonstrates the steady-state emission spectrum of MPHRP in the presence and absence of BHA. When BHA binds to MPHRP the emission spectrum shifts to higher wavelengths, and the fluorescence intensity is quenched. This enables the dissociation constant of the BHA−HRP complex to be determined by utilizing emission spectroscopy (*14*, *15*). In the inset of Figure 2, the binding curve of BHA to HRP in pH 5 is given. The value of $K_d = 51$ μM estimated from this curve is consistent with the literature values (*14*). Fluorescence lifetimes of the species (Table 1) have been determined, and they are consistent with literature values (*15*). The lifetimes do not change over the temperature range studied. For the experiments described below, we set the total concentration of BHA to be 250 μM so that the protein approaches saturation with BHA, and at the same time we avoid any possible denaturation by the alcohol and avoid the possibility of more than one BHA binding to the protein.

Table 1: Excited Singlet State and Triplet State Lifetimes of MPHRP in the Presence and Absence of BHA at Different Temperatures and Heavy Water[a]

temperature singlet (°C)	lifetime no BHA (ns)	lifetime with BHA (ns)	temperature triplet (°C)	triplet lifetime H_2O	triplet lifetime D_2O
35	18.39	17.56	35	$\tau_0 = 9.61$ $\tau = 0.77$	$\tau_0 = 22.18$ $\tau = 2.05$
25	18.45	17.76	20	$\tau_0 = 10.0$ $\tau = 1.38$	$\tau_0 = 23.87$ $\tau = 3.95$
15	18.68	17.72	5	$\tau_0 = 10.2$ $\tau = 2.63$	$\tau_0 = 24.2$ $\tau = 7.04$
5	18.86	18.12			

[a] pH = 5.

Long range motions in proteins occur in rather slow time scales. Excited triplet state lifetimes are in the correct time scale to monitor these motions. The relatively low quantum yield of the excited triplet state emission of MP limits its practical application as a probe of motion in the heme pocket. The excited triplet state of Pd-porphyrins is formed with high quantum efficiency (*32*). The steady state emission spectrum of Pd-MPHRP is depicted in Figure 4. The excited singlet state emission of Pd-MPHRP is very low as compared to the triplet and could only be observed by increasing the slits. Binding of BHA to the protein markedly quenches the excited triplet state of Pd-MPHRP. Although the quenching of the excited singlet state could not be well-characterized, it seemed to be much less than that of the excited triplet state, indicating that BHA is a much more efficient quencher of the excited triplet state. The lifetime of the excited singlet state was observed to be less than 100 ps, and its relative insensitivity toward BHA is likely to be due to this short lifetime. It is interesting to note that the spectrum of the triplet state of Pd-MPHRP is not distorted by BHA, while the spectrum of free base porphyrin is not only quenched but is also distorted by BHA as seen by the red shift (*14*).

In Figure 5, representative excited triplet state decay profiles of Pd-MPHRP in the presence and absence of BHA are given. Within the time frame that we observed, the excited triplet state exhibits monoexponential kinetics in the absence of BHA. In the presence of BHA, the triplet state decay profiles are biexponential, consisting of a short-lifetime component and a long-lifetime component that are equal to the decay of the unbound protein (Figure 5, inset). The preexponential factor for the long-lifetime component was less than 10% of the preexponential factor of the short-

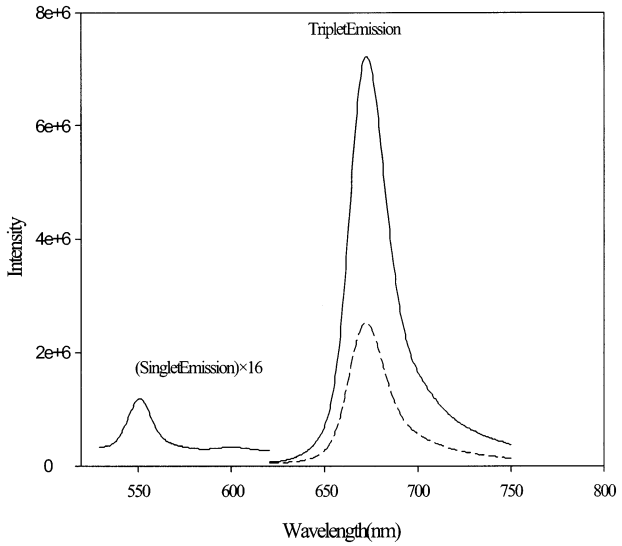

FIGURE 4: Steady-state emission of Pd-MPHRP in the absence (full line) and presence (dashed line) of BHA. The conditions were as follows: excitation was 396 nm, and emission and excitation bands were 1−1 nm for the triplet state and 2−2 nm for the singlet state emission. The protein concentration was 25 μM, the BHA concentration was 250 μM, the temperature is 25 °C, and the solvent was pH 5 ammonium acetate buffer (50 mM). The samples also contain deoxygenation reagents and were deoxygenated via the method described in Materials and Methods.

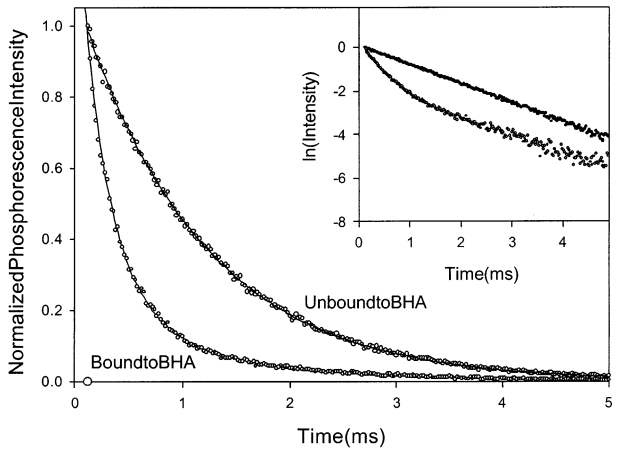

FIGURE 5: Triplet state decay profiles of Pd-MPHRP measured under free and BHA bound conditions. The symbols represent experimental values, and the solid lines represent exponential fits. From the exponential fit, lifetimes of 1.25 ms (no BHA) and 0.33 ms (bound to BHA) are obtained. The sample was excited at 394 nm, and the emission was collected at 675 nm. Both band-pass widths were set at 7 nm resolution. The points were collected at 0.05 ms intervals. The experiment was performed at 25 °C under the same sample conditions as Figure 3. The inset plots the natural log of the decay curves.

lifetime component. This is consistent with the residual unbound protein (see inset of Figure 3) at the BHA concentration that we have chosen.

Temperature and Medium Effects. We have investigated the effects of temperature, pH, and solvent deuterium isotopes upon the excited triplet state lifetime of Pd-MPHRP in the presence and absence of BHA. The results are tabulated in Tables 1−3. In Figure 6, Arrhenius plots for k' and $k_0 = \tau_0^{-1}$ are given for Pd-MPHRP. In the case of k_0, a small activation barrier is observed. This is consistent with phosphorescence and nonradiative intersystem crossing

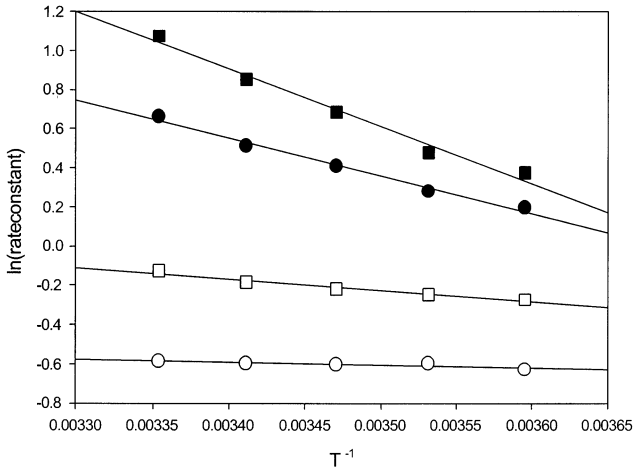

FIGURE 6: Arrhenius plots for Pd-MPHRP dissolved in H_2O (squares) and D_2O (circles). The sample conditions were the same as Figure 3. The full symbols are for k' and the open symbols are for k_0. For the rate constant k', the regression lines correlate with an activation energy of 5.8 kcal/mol (in water) and 3.8 kcal/mol (in heavy water), while for k_0 the activation energies are less than 0.5 kcal/mol for each of the two solvents.

(processes k_m and k_p in Figure 1) being the main routes for the relaxation of the excited triplet state as opposed to k_e. The rate constant k_0 does demonstrate a solvent kinetic isotope effect; for example, at 25 °C, the lifetime was 1.13 ms in H_2O and 1.79 ms in D_2O. This indicates that the process k_m is significant as compared to k_p. The fact that a solvent kinetic isotope effect is observed in the Pd porphyrin system that is devoid of exchangeable hydrogen atoms provides some evidence that it is possible that the nonradiative decay of the excited triplet state involves coupling to the water molecules existing in the heme pocket.

In contrast to k_0, the quenching rate constant k' is significantly temperature dependent (Figure 6). The viscosity of water remains relatively constant in the temperature range considered. At pH 5, the energy of activation is 5.8 kcal/mol for k'. The rate constant k' exhibits a solvent deuterium isotope effect. The energy of activation of k' in D_2O is 3.8 kcal/mol at pH 5. The quenching rate constants measured at $T = 25$ °C and pH = 5 are $k' = 2.96$ ms^{-1} (H_2O) and $k' = 1.94$ ms^{-1} (D_2O). The rate steadily decreases as the temperature decreases.

The k_0 and k' rate constants in Pd-MPHRP are depicted in Figure 7 for the pH values 5, 7, and 9. It appears that k_0 is pH independent, which is consistent with the fact that k_m and k_p are pH independent. Between pH 5 and 7, there was a sizable difference in the quenching constant. This difference is of interest and shall be discussed later.

In Figure 8, the Arrhenius plots for the rate constant k' of Pd-MPHRP have been given for different solvent systems. These plots are based upon the values tabulated in Table 2; the solvent viscosities are obtained from the literature (*39*). By increasing the solvent viscosity, the rate constant k' decreases steadily until it approaches a limiting value at high viscosity achieved at 60 and 70% glycerol and in the solid trehalose−sucrose glass. The scatter observed in the low temperature data points in the high viscosity solvents is expected because of the inherent uncertainty of 0.05 ms of the measurement conditions. In any case, it is reasonable to assume that all the high viscosity data are essentially

Table 2: Excited Triplet State Lifetimes (in ms) of Pd-MPHRP (τ_0) and Pd-MPHRP-BHA (t) in a Series of Different Solvents as a Function of Temperature and Viscosity[a]

T (°C)	H_2O	10% GW[b]	20% GW	30% GW	40% GW	50% GW	60% GW	70% GW	treh−glass	H_2O pH = 9	H_2O pH = 7	D_2O
25	$\tau_0 = 1.13$	$\tau_0 = 1.22$	$\tau_0 = 1.21$	$\tau_0 = 1.22$	$\tau_0 = 1.25$	$\tau_0 = 1.23$	$\tau_0 = 1.17$	$\tau_0 = 1.15$			$\tau_0 = 1.29$	$\tau_0 = 1.79$
	$\tau = 0.26$	$\tau = 0.32$	$\tau = 0.33$	$\tau = 0.37$	$\tau = 0.41$	$\tau = 0.48$	$\tau = 0.79$	$\tau = 0.61$			$\tau = 0.52$	$\tau = 0.40$
	(0.90cP)	(1.16cP)	(1.54cP)	(2.16cP)	(3.17cP)	(4.94cP)		***T* = 40 °C**				
20	$\tau_0 = 1.20$	$\tau_0 = 1.25$	$\tau_0 = 1.22$	$\tau_0 = 1.25$		$\tau_0 = 1.22$		$\tau_0 = 1.19$	$\tau_0 = 0.93$	$\tau_0 = 1.20$	$\tau_0 = 1.24$	$\tau_0 = 1.81$
	$\tau = 0.32$	$\tau = 0.35$	$\tau = 0.37$	$\tau = 0.42$		$\tau = 0.53$		$\tau = 0.71$	$\tau = 0.71$	$\tau = 0.41$	$\tau = 0.48$	$\tau = 0.45$
	(1.02cP)	(1.33cP)	(1.79cP)	(2.54cP)		(6.04cP)		***T* = 30 °C**				
15	$\tau_0 = 1.24$	$\tau_0 = 1.28$	$\tau_0 = 1.25$	$\tau_0 = 1.22$		$\tau_0 = 1.23$	$\tau_0 = 1.22$	$\tau_0 = 1.22$		$\tau_0 = 1.21$	$\tau_0 = 1.22$	$\tau_0 = 1.83$
	$\tau = 0.36$	$\tau = 0.41$	$\tau = 0.42$	$\tau = 0.45$		$\tau = 0.58$	$\tau = 0.91$	$\tau = 0.85$		$\tau = 0.45$	$\tau = 0.45$	$\tau = 0.49$
	(1.17cP)	(1.53cP)	(2.09cP)	(2.99cP)		(7.47cP)		***T* = 20 °C**				
10	$\tau_0 = 1.28$	$\tau_0 = 1.29$	$\tau_0 = 1.20$	$\tau_0 = 1.23$	$\tau_0 = 1.31$	$\tau_0 = 1.24$	$\tau_0 = 1.23$	$\tau_0 = 1.25$	$\tau_0 = 0.97$	$\tau_0 = 1.24$	$\tau_0 = 1.21$	$\tau_0 = 1.82$
	$\tau = 0.42$	$\tau = 0.46$	$\tau = 0.47$	$\tau = 0.51$	$\tau = 0.58$	$\tau = 0.64$	$\tau = 0.96$	$\tau = 0.94$	$\tau = 0.81$	$\tau = 0.50$	$\tau = 0.39$	$\tau = 0.53$
	(1.33cP)	(1.78cP)	(2.45cP)	(3.55cP)	(5.49cP)	(9.23cP)						
5	$\tau_0 = 1.31$	$\tau_0 = 1.32$	$\tau_0 = 1.30$	$\tau_0 = 1.24$	$\tau_0 = 1.27$	$\tau_0 = 1.26$	$\tau_0 = 1.23$			$\tau_0 = 0.56$	$\tau_0 = 1.18$	$\tau_0 = 1.88$
	$\tau = 0.45$	$\tau = 0.51$	$\tau = 0.54$	$\tau = 0.55$	$\tau = 0.61$	$\tau = 0.67$	$\tau = 1.02$			$\tau = 1.27$	$\tau = 0.36$	$\tau = 0.57$
	(1.54cP)	(2.06cP)	(2.88cP)	(4.24cP)	(6.67cP)	(11.50cP)						
0		$\tau_0 = 1.28$	$\tau_0 = 1.32$	$\tau_0 = 1.25$	$\tau_0 = 1.31$	$\tau_0 = 1.26$	$\tau_0 = 1.24$	$\tau_0 = 1.27$	$\tau_0 = 1.04$			
		$\tau = 0.55$	$\tau = 0.58$	$\tau = 0.58$	$\tau = 0.66$	$\tau = 0.77$	$\tau = 1.07$	$\tau = 1.04$	$\tau = 0.87$			
		(2.42cP)	(3.41cP)	(5.09cP)	(8.17cP)	(14.45cP)						
−5				$\tau_0 = 1.25$	$\tau_0 = 1.24$	$\tau_0 = 1.26$	$\tau_0 = 1.27$					
				$\tau = 0.67$	$\tau = 0.71$	$\tau = 0.81$	$\tau = 1.11$					
				(6.15cP)	(10.08cP)	(18.3cP)						
−10					$\tau_0 = 1.33$	$\tau_0 = 1.28$	$\tau_0 = 1.29$	$\tau_0 = 1.19$	$\tau_0 = 1.10$			
					$\tau = 0.78$	$\tau = 0.85$	$\tau = 1.13$	$\tau = 1.07$	$\tau = 0.92$			
					(12.54cP)							
						(23.39cP)						

[a]For each lifetime measured, the relevant solvent viscosity in cP is given in the parentheses below. [b] GW is an abbreviation for glycerol water mixture; the percent refers to the glycerol. Unless indicated, the pH = 5.

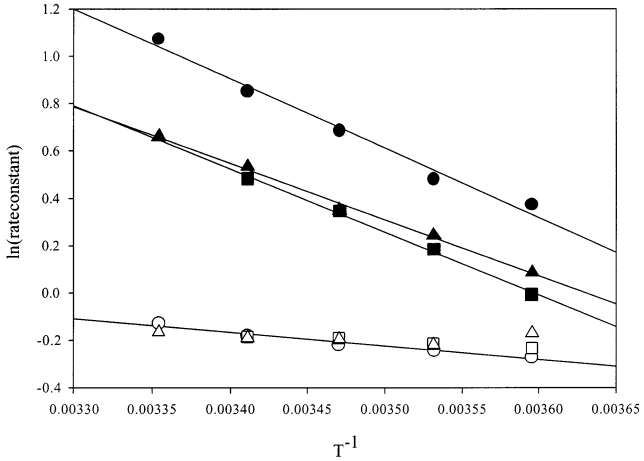

FIGURE 7: Arrhenius plots of k' (full symbols) and k_0 (open symbols) at different pH values. The circles are pH 5 (E_a = 5.8 kcal/mol), triangles are pH 7 (E_a = 4.7 kcal/mol), and the squares are pH 9 (E_a = 5.3 kcal/mol). No sizable temperature dependence for k_0 is observed. With the exception of the pH, all sample experimental conditions are identical with Figure 3.

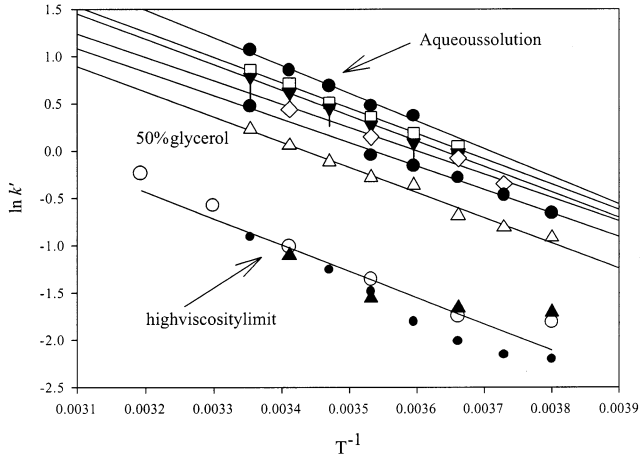

FIGURE 8: Arrhenius plots for the k' of Pd-MPHRP in solvents of different viscosity. The data from top to bottom are the k' values collected in 0, 10, 20, 30, 40, and 50% glycerol in water. The high viscosity data is represented by 60% glycerol (filled circles), 70% glycerol (open circles), and trehalose sugar glass (triangles). With the exception of glycerol content, all sample conditions are the same as Figure 3. The scatter observed in the high viscosity data is due to the uncertainty in the measured data. The correlation values for each of the data sets are given in Table 3.

identical, and we correlate the high viscosity data with a single straight line. These Arrhenius correlation lines values are given in Table 3. We have measured the effect of BHA at 77 K. At this temperature, no quenching of the phosphorescence was observed.

In Figure 9, the rate constant $(k'')^{-1}$ has been plotted as a function of viscosity. The correlation observed is highly linear, demonstrating that k'' is highly coupled with solvent friction. The quenching rate constant is in the order of $(ms)^{-1}$; therefore, the motions leading to quenching occur in the micro to millisecond time scale. These motions are relatively slow and correspond to long amplitude breathing motions of the protein.

In Figure 10, the ratio of N to M (eq 4) has been plotted as a function of temperature. This ratio represents internal friction and has the same units as viscosity. Judging from this parameter, it seems that the internal friction increases with decreasing temperature, and a range of values between 5 and 1.5 cP are obtained for this parameter.

DISCUSSION

Protein Dynamics. The quenching of Pd-MP phosphorescence by BHA can be considered to be a monitor of motion

Table 3: Fitting Parameters for the Arrhenius Plots ($\ln(k') = -E_a/RT + B$) Depicted in Figure 11[a]

solvent	E_a/R	B	$r^{2\,b}$	T (°C)	N	M	r^2
0%	2936.7	10.89	0.984	25	0.277	0.191	0.995
10%	2687.1	9.86	0.996	20	0.348	0.177	0.995
20%	2695.4	9.81	0.994	15	0.435	0.161	0.995
30%	2462.6	8.87	0.988	10	0.538	0.148	0.996
40%	2477.9	8.76	0.994	5	0.671	0.138	0.995
50%	2655.3	9.12	0.987				
high viscosity	2799.4	8.504	0.876				

[a] The percentages indicate glycerol in water and for the relationship $1/k'' = M\eta + N$ at different isotherms. [b] The correlation constant r^2 is given for all fits.

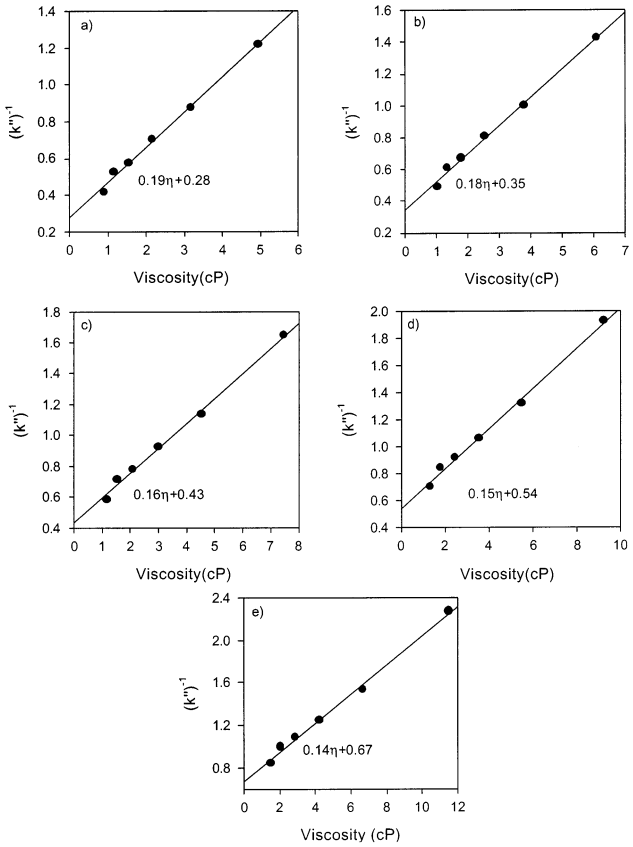

FIGURE 9: Dependence of $(k'')^{-1}$ as a function of viscosity at the isotherms (a) 25, (b) 20, (c) 15, (d) 10, and (e) 5 °C. The dashed lines are linear regression fits. The data are from Table 3 and Figure 8.

within the heme pocket. It is obvious that motion in the residues located on the surface of the protein is going to be highly solvent dependent. Motions in the interior of the protein are somewhat differently modulated by solvent.

The quenching of the fluorescence of MP−HRP by BHA does not exhibit any viscosity or temperature dependence, pointing to the fact that in the fluorescence lifetime only the BHA molecules that are close to the interaction sphere take part in the quenching reaction, and no motion is coupled with the excited singlet state quenching process. In contrast, the quenching of the excited triplet state with BHA has a significant temperature and viscosity dependence. This demonstrates that movement of the BHA and Pd-MP toward one another is in the same time scale as the Pd-MP excited triplet state lifetime.

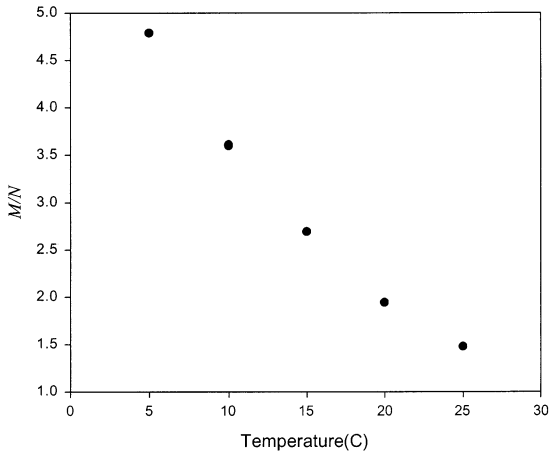

FIGURE 10: Ratio N/M as a function of temperature. The data are obtained from Figure 9 and fit according to eq 4.

The fact that the viscosity affects the triplet state lifetime of the Pd-MP demonstrates that the solvent modulates motion in the heme pocket. The interesting issue is that even in the highly viscous solvent systems, the activation energy is quite similar to the low viscosity solvent systems. This demonstrates that the entering of BHA into the interaction sphere is still the rate determining step in both high and low viscosity systems and that no large change in this mechanism is observed.

In our paper, we are examining the reaction between tightly bound moieties in one protein. The solvent viscosity dependence has been studied on systems such as protein−protein electron-transfer reactions (*40*−*43*) and the rebinding reaction of CO and the heme (*6*, *38*, *44*). In all cases referenced above, the solvent has a very large effect because of the fact that rather large amplitude protein motions are required for the reactions studied. In our case, the motions involved are not very large (not more than 0.4 nm), and yet the solvent can still influence motions of this amplitude in the interior of the protein.

Comments about the Quenching Mechanism. Although the quenching properties of BHA have been known for some time (*14*−*16*), the mechanism of energy transfer is not yet understood. Considering that there is no spectral overlap between BHA absorbance and porphyrin emission, Foerster type energy transfer is ruled out as a possibility (*45*). An alternative quenching mechanism may be electron transfer. Of course, the most unambiguous way of verifying electron transfer is to observe the charged species via transient absorbance measurements. However, some of our measurements are consistent with electron-transfer being the quenching mechanism. First, BHA is a good reducing agent (*46*, *47*), while porphyrins can both be reduced and oxidized (*48*). Second, the oxidation of BHA in aqueous media involves the loss of a proton, and this can give rise to the solvent kinetic isotope effect that we have observed. Third, BHA has its maximum reducing power at pH values close to 6 (*47*), and this is consistent with the pH dependence observed for the quenching rate constant.

We note that our results are consistent with the sphere of action model. Electron transfer, of course, occurs through a distance. A further refinement of the kinetic model would be to incorporate a distance dependence in the model. It is likely, however, that the fits would not be very different.

Some degree of orbital overlap is required for electron transfer, and the distance dependence of interaction is quite steep. Therefore, the reaction of the molecules at the closest distance is always predominant, and when there is motion (once the molecule moves to a favorable position) reaction occurs. Consistent with this model is also the fact that in equilibrium position in the absence of motion (i.e., at 77 K), quenching does not occur.

In summary, we have demonstrated that the active site of the enzyme horseradish peroxidase has dynamic motion in the micro to millisecond time scale and that this motion is affected by the solvent. We also suggest that the mechanism that BHA quenches the porphyrin emission might be electron transfer from BHA to the porphyrin.

ACKNOWLEDGMENT

The authors would like to acknowledge interesting and informative discussions that they have had with Dr. Chris Moser from the University of Pennsylvania in the field of electron transfer. We would also like to acknowledge an informative discussion about Kramers theory with Prof. Susan Tucker from UC−Davis. The technical support of Mr. Wayne Wright is gratefully acknowledged.

REFERENCES

1. Marcus, R. A. (1997) *Pure App. Chem. 69*, 13−29.
2. Barbara, P. F., Meyer, T. J., and Ratner, M. A. (1996) *J. Phys. Chem. 100*, 13148−13168.
3. Moser, C. C., Keske, J. M., Warncke, K., Farid, R. S., and Dutton, P. L. (1992) *Nature 355*, 796−802.
4. Closs, G. L., and Miller, J. R. (1988) *Science 240*, 440−447.
5. Verhoeven, J. W. (1999) *Adv. Chem. Phys. 106*, 603−644.
6. Frauenfelder, H., Petsko, G. A., and Tsernoglou, D. (1979) *Nature 280*, 558−563.
7. Steinfeld, J. I., Francisco, J. S., and Hase, W. L. (1999) *Chemical Kinetics Dynamics*, 2nd ed., Prentice Hall, Upper Saddle River, NJ.
8. Kramers, H. A. (1940) *Physica 7*, 284−304.
9. Tucker, S. C. (2000) *Theor. Chem. Acc. 103*, 209−211.
10. Chance, B. (1952) *Arch. Biochem. Biophys. 41*, 416−424.
11. George, P. (1953) *Biochem. J. (London) 55*, 220−230.
12. Morishima, I., and Ogawa, S. (1979) *J. Biol. Chem. 254*, 2814−2820.
13. Schonbaum, G. R. (1973) *J. Biol. Chem. 248*, 502−511.
14. Aviram, I. (1981) *Arch. Biochem. Biophys. 212*, 483−490.
15. Horie, T., Vanderkooi, J. M., and Paul, K. G. (1985) *Biochemistry 24*, 7935−7941.
16. Fidy, J., Paul, K. G., and Vanderkooi, J. M. (1989) *Biochemistry 28*, 7531−7541.
17. Veitch, N. C., and Williams, R. J. P. (1995) *Eur. J. Biochem. 229*, 629−640.
18. Indiani, C., Feis, A., Howes, B. D., Marzocchi, M. P., and Smulevich, G. (2000) *J. Am. Chem. Soc. 122*, 7368−7376.
19. Smulevich, G., Paoli, M., Burke, J. F., Smith, A. T., Sanders, S. A., and Thorneley, R. N. F. (1994) *Biochemistry 33*, 7398−7407.
20. Smulevich, G., English, A. M., Mantini, A. R., and Marzocchi, M. P. (1991) *Biochemistry 30*, 772−779.
21. Smulevich, G., Feis, A., Indiani, C., Becucci, M., and Marzocchi, M. P. (1999) *J. Biol. Inorg. Chem. 4*, 39−47.
22. Chang, Y.-T., Veitch, N. C., and Loew, G. H. (1998) *J. Am. Chem. Soc. 120*, 5168−5178.
23. Henriksen, A., Schuller, D. J., Meno, K., Welinder, K. G., Smith, A. T., and Gajhede, M. (1998) *Biochemistry 37*, 8054−8060.
24. La Mar, G. N., Hernandez, G., and De Ropp, J. S. (1992) *Biochemistry 31*, 9158−9168.
25. De Ropp, J. S., Mandal, P. K., and La Mar, G. N. (1999) *Biochemistry 38*, 1077−1086.
26. Gilfoyle, D. J., Rodriguez-Lopez, J. N., and Smith, A. T. (1996) *Eur. J. Biochem. 236*, 714−722.
27. Aitken, S. M., Turnbull, J. L., Percival, M. D., and English, A. M. (2001) *Biochemistry 40*, 13980−13989.
28. Rakhit, G., and Chignell, C. F. (1979) *Biochim. Biophys. Acta 580*, 108−119.
29. Rich, P. R., Wiegand, N. K., Blum, H., Moore, A. L., and Bonner, W. D., Jr. (1978) *Biochim. Biophys. Acta 525*, 325−337.
30. Leigh, J. S., Maltempo, M. M., Ohlsson, P. I., and Paul, K. G. (1975) *FEBS Lett. 51*, 304−308.
31. Lakowicz, J. R. (1983) *Principles of Fluorescent Spectroscopy*, Plenum Press, New York.
32. Eastwood, D., and Gouterman, M. (1970) *J. Mol. Spectrosc. 35*, 359−375.
33. Papp, S., Vanderkooi, J. M., Owen, C. S., Holtom, G. R., and Phillips, C. M. (1990) *Biophys. J. 58*, 177−186.
34. Zelent, B., Kusba, J., Gryczynski, I., Johnson, M. L., and Lakowicz, J. R. (1996) *J. Phys. Chem. 100*, 18592−18602.
35. Vanderkooi, J. M., Moy, V. T., Maniara, G., Koloczek, H., and Paul, K. G. (1985) *Biochemistry 24*, 7931−7935.
36. Horie, T., and Vanderkooi, J. M. (1982) *FEBS Lett. 147*, 69−73.
37. Wright, W. W., Baez, J. C., and Vanderkooi, J. M. (2002) *Anal. Biochem. 307*, 167−172.
38. Ansari, A., Jones, C. M., Henry, E. R., Hofrichter, J., and Eaton, W. A. (1992) *Science 256*, 1796−1798.
39. CRC (1958) *Handbook of Chemistry and Physics*, 40th ed., Chemical Rubber Publishing Co., Cleveland, OH.
40. Mei, H., Wang, K., Peffer, N., Weatherly, G., Cohen, D. S., Miller, M., Pielak, G., Durham, B., and Millett, F. (1999) *Biochemistry 38*, 6846−6854.
41. Oh-oka, H., Iwaki, M., and Itoh, S. (1997) *Biochemistry 36*, 9267−9272.
42. Crnogorac, M. M., Shen, C., Young, S., Hansson, O., and Kostic, N. M. (1996) *Biochemistry 35*, 16465−16474.
43. Ivkovic-Jensen, M. M., and Kostic, N. M. (1997) *Biochemistry 36*, 8135−8144.
44. Frauenfelder, H., Sligar, S. G., and Wolynes, P. G. (1991) *Science 254*, 1598−1603.
45. Turro, N. J. (1978) *Modern Molecular Photochemistry*, University Science Books, Mill Valley, CA.
46. Rowe, J. E., and Ward, A. D. (1968) *Aust. J. Chem. 21*, 2761−2767.
47. Gillam, A. H., Lewis, A. G., and Andersen, R. J. (1981) *Anal. Chem. 53*, 841−844.
48. Dolphin, D. (1978) *The Porphyrins, Vol. 5: Physical Chemistry, Pt. C*, Academic Press, New York.

BI020325N